INTERNATIONAL SOCIETY FOR SOIL MECHANICS AND GEOTECHNICAL ENGINEERING

IS-PORTO 2023 PROCEEDINGS

Proceedings of the 8th International Symposium on
DEFORMATION CHARACTERISTICS OF GEOMATERIALS
Porto, 3rd - 6th September 2023

Temperature-dependent elastic shear modulus of a saturated lateritic clay

Obed Takyi Bentil[1], Chao Zhou[1#], Daniel Peprah-Manu[2] and Damilola Bashir Akinniyi[3]

[1]*Department of Civil and Environmental Engineering, The Hong Kong Polytechnic University, Hung Hom, Hong Kong*
[2]*Department of Civil and Environmental Engineering, The Hong Kong University of Science and Technology, Clear Water Bay, Kowloon, Hong Kong*
[3]*Department of Civil Engineering, Coventry University, Coventry, UK*
[#]*Corresponding author: c.zhou@polyu.edu.hk*

ABSTRACT

The thermo-mechanical behaviour of saturated clays and sands has been studied by many researchers, considering that it is useful in many geotechnical problems, such as the analysis of energy foundations and the effects of climate change on earth structures. Despite the fact that temperature is known to affect the yielding and volume change behaviour of soils, the effects of temperature on the elastic shear modulus (G_0) of soils are rarely studied. In this study, a temperature-controlled oedometer equipped with bender elements was developed. It was used to investigate the effects of temperature on G_0 of a compacted lateritic clay at saturated conditions. The G_0 was measured at 5 and 40°C during loading and unloading in the stress range of 30 to 400 kPa. Four tests were conducted in which two different initial densities (95% and 85% of maximum dry density (MDD) were considered. The results will be interpreted and discussed with reference to the elastoplastic modelling of thermo-mechanical soil behaviour.

Keywords: temperature, elastic shear modulus, lateritic soil, clays.

1. Introduction

In recent years, the thermo-mechanical response of soils has garnered a lot of attention due to their significance to several developing study fields like energy geo-structures (Laloui & Di Donna, 2013; McCartney et al., 2016). However, the majority of earlier studies concentrated on how temperature affected soil's shear strength, yielding, and thermal strain (Abuel-Naga et al., 2007; Cekerevac & Laloui, 2004; Graham et al., 2001; Hueckel & Baldi, 1990; Ng et al., 2019b; Pan et al., 2020).

The effect of temperature on soil stiffness, which is essential for analysing the serviceability limit condition of energy piles, subsurface thermal energy storage facilities, etc., has received very little attention up to this point. By considering various overconsolidation ratios (OCRs), the temperature-dependent secant Young's modulus of a saturated kaolin clay at axial strain of 0.5%, was determined by Cekerevac and Laloui (2004). It was found that the secant modulus at each OCR slightly increased when the temperature rose from 22 to 90°C. Zhou et al. (2015) determined the secant shear modulus of a silt in the strain range of 0.003% to 1%. The modulus at 60°C was consistently lower than that at 20°C when the deviator strain was less than 0.3%, and the difference diminished as the deviator strain increased. The literature has emerged with contradictory findings that cannot be well explained using the influence of OCR. The discrepancy could be explained by the variations in stress conditions, temperatures, and strains between the two studies (Bentil & Zhou, 2022). Moreover, the initial density or void ratio, which has an influence on thermo-mechanical behaviour has not been considered entirely. In addition, soil mineralogy has been reported to affect saturated soils' thermo-mechanical behaviour (Abuel-Naga et al., 2007; Ng et al., 2020). The effects of such minerals on the thermo-mechanical behaviour of saturated soils at different void ratios are rarely reported, especially for residual lateritic soils rich in sesquioxide.

This paper investigates the influence of the initial void ratio on G_0 of compacted soil with different temperatures and stress using a temperature-controlled oedometer equipped with bender elements. One-dimensional compression tests were performed on saturated compacted lateritic clay soil rich in sesquioxide prepared with two different void ratios or densities. Measurements of G_0 during the compression at two different temperatures are presented and discussed.

2. Methodology

2.1. Testing Apparatus

Tests were conducted with a new temperature-controlled oedometer equipped with bender elements developed by Bentil and Zhou (2022), as shown in Figure 1. The apparatus is equipped with a temperature control system manufactured by PolyScience that controls the temperature from −20°C to 170°C. To control soil temperature, water was heated or cooled in a spiral copper tube surrounding the specimen and monitored by two thermocouples installed within the soil specimen (at the centre and end of the specimen), and one thermocouple installed outside the specimen and within

the oedometer. The installed bender elements were used to measure shear wave velocity during the test, to estimate the G_0 of the soil. The apparatus was calibrated to evaluate the influence of the temperature cycles on the measurement devices before any tests were conducted. Further details on the new temperature-controlled oedometer apparatus can be found in Bentil and Zhou (2022). Several calibration exercises noted that the bender element system worked better in temperatures lower than 60°C. Therefore, all tests in this study were conducted at temperatures lower than 60°C.
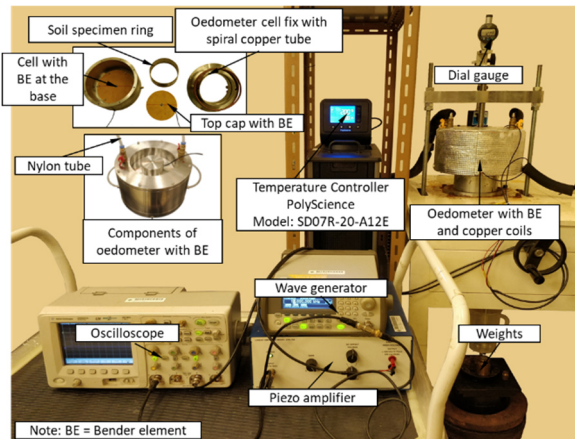
Figure 1. Temperature-controlled oedometer equipped with bender elements.

2.2. Test Soil, Program, and Procedures

A lateritic clay soil rich in sesquioxide, whose detailed description is reported by (Ng et al., 2019a) was used in this study. Figure 2 shows the particle size distribution curve of the lateritic clay soil. According to the Unified soil classification system (USCS), this soil is classified as a Sandy lean clay (CL) (ASTM, 2017). The basic properties of the test soil including the mineral composition reported by Ng et al. (2020) are summarised in Table 1. The liquid limit was obtained using the Fall-cone penetration method.
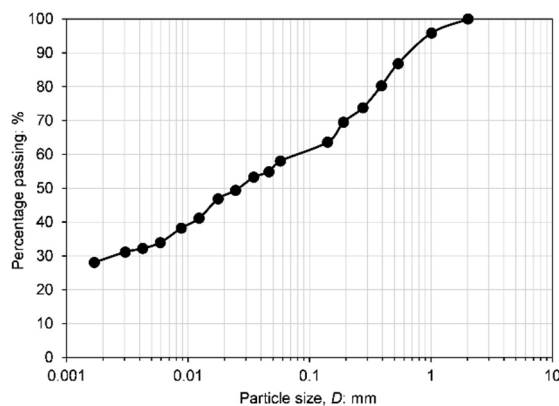
Figure 2. Grain size distribution curve of lateritic clay soil

The test specimens were statically compacted at the optimum water content (19.5%) to two target densities of 0.85 and 0.65, corresponding to 85% and 95% maximum dry density (MDD). The diameter and height of each test specimen were controlled to 150 and 60 mm, respectively. After static compaction to the initial target void ratios was completed, the test specimens were

submerged in de-aired water under nominal effective stress of about 12 kPa for at least 48 h to saturate. A small vacuum was applied to the top of the saturation flask to remove any air bubbles within the specimens to help achieve full saturation.

After saturation, the specimens were set up in the oedometer apparatus under initial affective stress of 30 kPa and tested. Figure 3 shows the stress path followed during the test. One-dimensional (1D) compression tests were performed at two pre-defined temperatures of 5°C and 40°C. These two temperature values were selected in this study to simulate decreasing or increasing temperatures respectively, due to climate change action in tropical and relatively humid regions in the world. This is to show how the mechanical behaviour of the lateritic clay soil would be affected by changes in temperature due to climate change effects.

Table 1. Physical properties of the lateritic clay soil

Index property	Value
Atterberg Limits (%)	
• Liquid limit	47
• Plastic limit	26
• Plasticity index	21
Particle size distribution (%)	
• Sand fraction	42
• Silt fraction	30
• Clay fraction	28
Standard proctor compaction	
• Optimum water content (%)	19.5
• Maximum dry density (Mg/m³)	1.7
Main mineral composition (%)	
• Quartz	65
• Hematite	17
• Goethite	9
• Kaolinite	9
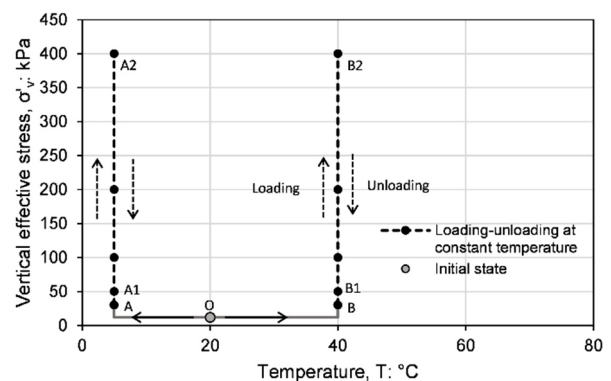
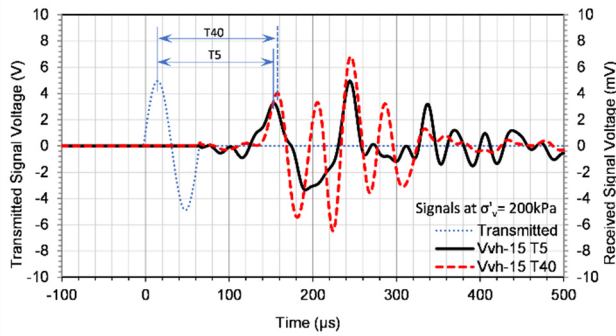**Figure 3.** Thermo-mechanical stress paths

Table 2. Summary of the initial state of test specimens

Test ID	w: %	e	T: °C	σ'$_v$: kPa
e0.85-T5		0.85	5	
e0.85-T40	19.5		40	30, 50, 100, 200 & 400
e0.65-T5		0.65	5	
e0.65-T40			40	

w = initial water content, e = initial void ratio, T = temperature, σ'$_v$ = vertical effective stress

Figure 4. Example of bender element test results for at different temperatures at constant vertical effective stress of 200 kPa.

In each test, a pre-defined temperature was first applied to the specimen by either reducing the room temperature shown by the stress path O-A from 20°C to 5°C or by increasing the room temperature from 20°C to 40°C through stress path O-B. To ensure that test specimens reached thermal equalisation, the thermocouples were monitored for at least 12 h until there were no significant changes in the temperature readings of the specimens. In addition, dial gauge readings were monitored to evaluate any vertical deformations during the thermal equalisation stage. After the test specimen had reached thermal equalisation (no significant changes in temperature and vertical deformation), the vertical effective stress was increased in a stepwise manner from 30 to 400 kPa (A-A2 or B-B2), which constitutes the loading stage, followed by a stepwise unloading stage from 400 kPa to 30 kPa (A2-A or B2-B). The consolidation process in each stage was considered to have reached equilibrium when the dial gauge reading stayed constant for at least 24 h. At each desired equilibrium thermomechanical state indicated by round and black solid markers in Figure 3, bender element tests were performed to measure the shear wave velocity to estimate G_0 during loading and unloading. Figure 4 shows an example of the transmitted and received signals at 5°C and 40°C. A piezo amplifier with a 20-times voltage amplification capacity was used to transmit a sine wave pulse with a 5V voltage level to the transmitter bender elements. So, this bender element received an excitation voltage of 100V peak to peak. This voltage is considerably lower than the bender element's peak voltage to keep the bender element from depolarising. Based on the typical frequencies mentioned in the literature, the input frequency was set to 20 kHz (Lee & Santamarina, 2005; Leong et al., 2009). From Figure 4, it can be deduced that the travel time from the transmitter to the receiver bender element is affected by the temperature. This may be due to not only the density or void ratio but also the nature of the particle contacts to transmit the shear waves. A summary of the initial test details of the specimens is shown in Table 2.

3. Experimental results

Figure 5 shows the results of the influence of temperature on 1-D compression for (a) medium-dense saturated lateritic clay, and (b) densely compacted of saturated lateritic clay at 5°C and 40°C, respectively.

From Figure 5(a), at each temperature, there is an initial gradual decrease in the void ratio after loading, until the pre-yield stress is reached. After that, any loading causes significant compression to the compacted specimen until maximum stress of 400 kPa is reached. The figure shows that the void ratio at 40°C is larger than the void ratio at 5°C during compression after yielding. This may suggest that at that compaction density, the effects of temperature on the solid minerals are insignificant to its compression behaviour. The pre-consolidation pressure for both specimens at different temperatures was estimated to be around 50 kPa, however the pre-consolidation pressure of 5°C is likely less than that of 40°C. After compression, the specimens were unloaded through a stepwise method of reducing the load from 400 kPa to 30 kPa to evaluate the effects of temperature on the unloading-reloading line (URL). For the medium-dense states, the URL is not affected by temperature variations. Similar trend has been reported by previous authors (Campanella & Mitchell, 1968). As can be seen from Figure 5(a), the compression line of medium dense soil shifts to the right with an increase in temperature. Since the elastic zone is defined as the range of void ratio against vertical stress values that falls within the boundary of the unloading-reloading line and normal compression line, Figure 5(a) is an indication of an increase in the elastic zone at high temperatures for the loose specimen. This behaviour is contradictory from what has been reported previously in the literature (Abuel-Naga et al., 2007; Cheng et al., 2020).

Figure 5(b) on the other hand shows the compression behaviour of the densely compacted specimens at 5°C and 40°C. The compressibility behaviour before yielding (at stresses below 200 kPa) is very similar for specimens prepared at 5°C and 40°C. After 200 kPa vertical effective stress, the compression line at 40°C tends to move towards the left side. In other words, after seemingly yielding (around 200 kPa), the compressibility of the dense specimen at 40°C seems to be higher than the compressibility of the dense specimen at 5°C. Similar results has been reported in the literature by other researchers (Abuel-Naga et al., 2007; Cheng et al., 2020). Due to the sample size, there is a limitation on the compression machine to apply higher stresses beyond 400 kPa. Hence, the pre-consolidation pressure or yield stress could not be determined rigorously. However, due to a shift in compression line to the left side, it can be preliminary assumed that the elastic region shrinks when temperature increases to 40°C. The URL of the dense specimens was also evaluated and found not to be significantly affected by temperature variations, since during unloading, the two specimens show a similar swelling characteristic.

In comparison, the pre-consolidation pressure of the dense states is increased by at least 320% compared to the medium-dense states, independent of the thermal state. This increase in pre-consolidation pressure could be due to the higher initial stress required to achieve the initial void ratio of 0.65 as compared to that required to achieve a void ratio of 0.85 for the medium-dense states.
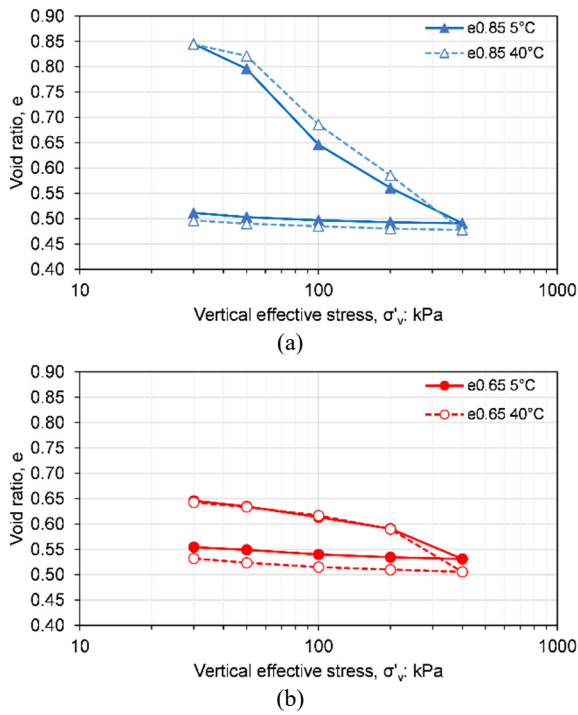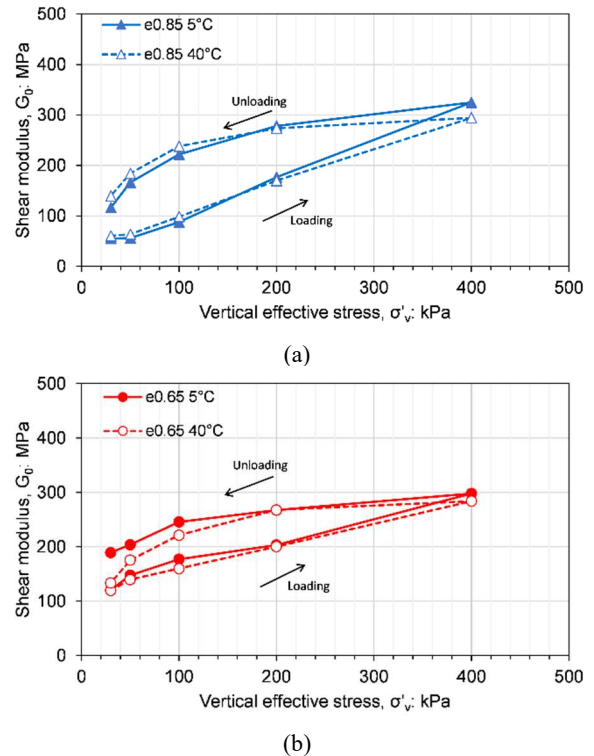
Figure 5. Influence of temperature on 1D compression for (a) medium dense, and (b) densely compacted specimens

To fully evaluate the effects of temperature on compressibility characteristics, the shear modulus was estimated at each thermo-mechanical state. Figure 6 shows the influence of temperature on the maximum shear modulus of medium-dense (Figure 6(a)) and dense (Figure 6(b)) compacted specimens. From Figure 6(a) (medium dense state), at each temperature, the shear modulus increases monotonically up to 400 kPa vertical stress during loading. During unloading, there is a reduction in shear modulus with decreasing stress. However, at each constant vertical stress state, the shear modulus of the unloading stage is significantly higher than the shear modulus at the loading stage. This could be due to the difference in void ratio for similar stress states along the loading and unloading curves. Figure 5(a) shows that for the same vertical stress, the void ratio during unloading is significantly lower than the void ratio during loading, which could be the reason for the higher stiffness during unloading in Figure 6(a) as compared to the loading stage. Since the void ratio is smaller during unloading, the specimen is much dense and much stiffer, resulting in a higher shear modulus.

When the specimens are compared at each temperature, it can be seen that the G_0 at 40°C are consistently higher than those at 5°C during both loading and unloading, except at 400 kPa vertical stress, even though the void ratio slightly lower at 5°C, during loading stage. This result is unexpected but possible because of the thermal effects on soil yield stress. It appears that, the medium dense soil may be experiencing thermal hardening (i.e., initial increase in the yield stress as temperature increases). Hence, due to thermal hardening effects, the stiffness increases with increasing temperature. The maximum difference in G_0 between 5°C and 40°C is about 22% during loading, and 20% during unloading. It can also be seen from the figure that irrespective of the temperature, there seems to be a gradual decrease in G_0 during unloading between 400 kPa and 200 kPa, accompanied by a sharp decrease in G_0 at stresses below 200 kPa. It can be inferred from the figure that heating generally increases G_0 during loading and unloading at vertical stresses below 200 kPa when the soil is compacted at a medium-dense state. The maximum difference in G_0 between loading and unloading for the medium-dense specimens is about 200%. The new results of this study suggest that the significance of thermal effects is stress path dependent.

For the densely compacted specimens, Figure 6(b) shows their shear modulus behaviour during loading and unloading at two different thermal states. The G_0 behaviour during loading and unloading is similar to what was previously discussed for the medium-dense specimens, with an increase in G_0 during loading, followed by a decrease in G_0 during unloading. However, in this case, the specimens at 5°C seem to consistently have a higher G_0 during loading and unloading when compared with 40°C, even though the specific volume is lower at 40°C because of the thermal effects on soil compressibility.

Figure 6. Influence of temperature on the maximum shear modulus of (a) medium-dense and (b) densely compacted specimens

The maximum difference in G_0 between specimens at 5°C and 40°C during loading is about 10% (see the data points at 100 kPa), whiles during unloading, the maximum difference is up to 30% (at 30 kPa). In addition, at each vertical stress state, the difference between the shear modulus at loading and the shear modulus at unloading is far smaller as compared to the medium-dense specimens in Figure 6(a). This behaviour is also independent of temperature. This larger shear modulus hysteresis in medium-dense specimens could be due to the higher void ratio, representing a much larger pore volume accompanied by minimum particle contact.

It is insightful to note that for densely compacted specimens, an increase in temperature consistently decreases the G_0, contrary to what was previously reported for medium-dense specimens (increasing temperature increases G_0). The decrease in G_0 with temperature for the densely compacted specimens can be attributed to the influence of temperature on the interparticle force of saturated clay (Laloui, 2001). As suggested by the double layer theories (Israelachvili, 2011), an increase in soil temperature would increase the electrical repulsive force between soil particles, thereby causing a reduction of G_0.

4. Discussion

Some important findings can be drawn from the preceding section. Firstly, changes in G_0, with an increase in temperature seem to be affected by the initial density of the soil. Although, a decrease in G_0 with temperature may be attributed to the influence of temperature on the interparticle force of saturated clay through an increase in repulsive force between soil particles (Israelachvili, 2011; Laloui, 2001).

The interpretation above may no longer be applicable when factors such as variable particle contact stress caused by different initial densities and whether the soil is experiencing thermal hardening or softening come into play. There are possibly competing effects for the reduction of inter-particle contact due to temperature by different initial densities. It seems possible that when the sample is dense, the interparticle contact reduction due to temperature is more significant than when the sample becomes less dense. Besides the effect of OCR, more experimental results may be required for thermal effects on different soil types prepared at different densities.

5. Conclusions

Temperature variations seem to affect the compressibility characteristics of densely compacted specimens, with the compressibility increasing as temperature increases. On the contrary, there seem to be no significant changes in compressibility behaviour with temperature changes for medium-dense compacted states.

During 1D compression, the shear modulus increased with increasing vertical stress during loading and reduced during unloading as expected. This is due to the reduction in the void ratio and the increase in inter-particle contacts during loading, and vice versa during unloading. This behaviour was consistent and independent of the temperature variations.

When the temperature is increased for medium-dense compacted specimens, there is a subsequent increase in the shear modulus during loading and unloading, especially at vertical stresses lower than 200 kPa. On the contrary, for densely compacted specimens, increasing temperature reduced the shear modulus during loading and unloading. For the densely compacted specimens, the shear modulus decreases with temperature due to the reduction in inter-particle forces with temperature as a result of the increase in electrical double-layer repulsive forces.

In summary, heating reduces G_0 in overconsolidated soils as the soil experiences thermal softening and increases G_0 in normally consolidated soils as the soil experiences thermal hardening. Moreover, thermal hardening or softening may occur in a soil depending on the density and possibly structural characteristics of the soil, causing an increase or decrease in shear modulus during hearing. More research is needed to explore the influence of initial density and structural characteristics on the temperature-dependent shear modulus of other soil. These results provide experimental evidence to improve the current thermomechanical constitutive models.

References

Abuel-Naga, H. M., Bergado, D. T., Bouazza, A., & Ramana, G. V. (2007). Volume change behaviour of saturated clays under drained heating conditions: experimental results and constitutive modeling. *Canadian Geotechnical Journal*, *44*, 942-956. https://doi.org/10.1139/t07-031

ASTM. (2017). D2487 − 17e1: Standard Practice for Classification of Soils for Engineering Purposes (Unified Soil Classification System). In. West Conshohocken, Pa. USA: ASTM International.

Bentil, O. T., & Zhou, C. (2022). Effects of Temperature and Thermal Cycles on the Elastic Shear Modulus of Saturated Clay. *Journal of Geotechnical and Geoenvironmental Engineering*, *148*. https://doi.org/10.1061/(ASCE)GT.1943-5606.0002822

Campanella, R. G., & Mitchell, J. K. (1968). Influence of Temperature Variations on Soil Behavior. *Journal of the Soil Mechanics and Foundations Division*, *94*(3), 709-734. https://doi.org/10.1061/jsfeaq.0001136

Cekerevac, C., & Laloui, L. (2004). Experimental study of thermal effects on the mechanical behaviour of a clay. *International Journal for Numerical and Analytical Methods in Geomechanics*, *28*, 209-228. https://doi.org/10.1002/nag.332

Cheng, Q., Zhou, C., Ng, C. W. W., & Tang, C. (2020). Effects of soil structure on thermal softening of yield stress. *Engineering Geology*, *269*, 105544.

Graham, J., Tanaka, N., Crilly, T., & Alfaro, M. (2001). Modified Cam-Clay modelling of temperature effects in clays. *Canadian Geotechnical Journal*, *38*, 608-621. https://doi.org/10.1139/cgj-38-3-608

Hueckel, T., & Baldi, G. (1990). Thermoplasticity of Saturated Clays: Experimental Constitutive Study. *Journal of Geotechnical Engineering*, *116*, 1778-1796. https://doi.org/10.1061/(ASCE)0733-9410(1990)116:12(1778)

Israelachvili, J. (2011). Intermolecular and surface forces. In (3rd ed.). New York: 3rd Edition. Academic Press.

Laloui, L. (2001). Thermo-mechanical behaviour of soils. *Revue Française de Génie Civil*, *5*(6), 809-843. https://doi.org/10.1080/12795119.2001.9692328

Laloui, L., & Di Donna, A. (2013). Energy Geostructures. In L. Laloui & A. Di Donna (Eds.), *Energy Geostructures:*

Innovation in Underground Engineering (pp. 1-304). Hoboken, NJ USA: John Wiley & Sons, Inc.

Lee, J.-S., & Santamarina, J. C. (2005). Bender Elements: Performance and Signal Interpretation. In *Journal of Geotechnical and Geoenvironmental Engineering* (Vol. 131, pp. 1063-1070).

Leong, E. C., Cahyadi, J., & Rahardjo, H. (2009). Measuring shear and compression wave velocities of soil using bender–extender elements. In *Canadian Geotechnical Journal* (Vol. 46, pp. 792-812).

McCartney, J. S., Sánchez, M., & Tomac, I. (2016). Energy geotechnics: Advances in subsurface energy recovery, storage, exchange, and waste management. In *Computers and Geotechnics* (Vol. 75, pp. 244-256): Elsevier Ltd.

Ng, C. W. W., Akinniyi, D. B., & Zhou, C. (2020). Volume change behaviour of a saturated lateritic clay under thermal cycles. In *Bulletin of Engineering Geology and the Environment* (Vol. 80, pp. 653-661).

Ng, C. W. W., Akinniyi, D. B., Zhou, C., & Chiu, C. F. (2019a). Comparisons of weathered lateritic, granitic and volcanic soils: Compressibility and shear strength. *Engineering Geology*, *249*, 235-240. https://doi.org/10.1016/j.enggeo.2018.12.029

Ng, C. W. W., Mu, Q. Y., & Zhou, C. (2019b). Effects of specimen preparation method on the volume change of clay under cyclic thermal loads. In *Géotechnique* (Vol. 69, pp. 146-150).

Pan, Y., Coulibaly, J. B., & Rotta Loria, A. F. (2020). Thermally induced deformation of coarse-Fgrained soils under nearly zero vertical stress. In *Géotechnique Letters* (Vol. 10, pp. 486-491).

Zhou, C., Xu, J., & Ng, C. W. W. (2015). Effects of temperature and suction on secant shear modulus of unsaturated soil. In *Géotechnique Letters* (Vol. 5, pp. 123-128).